DOI: 10.1002/chem.200500896

A Two-State Computational Investigation of Methane C–H and Ethane C–C Oxidative Addition to $[CpM(PH_3)]^{n+}$ (M = Co, Rh, Ir; $n = 0, 1$)

Alban Petit,[a] Philippe Richard,[a] Ivo Cacelli,[b] and Rinaldo Poli*[c]

Abstract: Reductive elimination of methane from methyl hydride half-sandwich phosphane complexes of the Group 9 metals has been investigated by DFT calculations on the model system $[CpM(PH_3)(CH_3)(H)]$ (M = Co, Rh, Ir). For each metal, the unsaturated product has a triplet ground state; thus, spin crossover occurs during the reaction. All relevant stationary points on the two potential energy surfaces (PES) and the minimum energy crossing point (MECP) were optimized. Spin crossover occurs very near the σ-CH_4 complex local minimum for the Co system, whereas the heavier Rh and Ir systems remain in the singlet state until the CH_4 molecule is almost completely expelled from the metal coordination sphere. No local σ-CH_4 minimum was found for the Ir system. The energetic profiles agree with the non-existence of the Co^{III} methyl hydride complex and with the greater thermal stability of the Ir complex relative to the Rh complex. Reductive elimination of methane from the related oxidized complexes $[CpM(PH_3)(CH_3)(H)]^+$ (M = Rh, Ir) proceeds entirely on the spin doublet PES, because the 15-electron $[CpM(PH_3)]^+$ products have a doublet ground state. This process is thermodynamically favored by about 25 kcal mol^{-1} relative to the corresponding neutral system. It is essentially barrierless for the Rh system and has a relatively small barrier (ca. 7.5 kcal mol^{-1}) for the Ir system. In both cases, the reaction involves a σ-CH_4 intermediate. Reductive elimination of ethane from $[CpM(PH_3)(CH_3)_2]^+$ (M = Rh, Ir) shows a similar thermodynamic profile, but is kinetically quite different from methane elimination from $[CpM(PH_3)(CH_3)(H)]^+$: the reductive elimination barrier is much greater and does not involve a σ-complex intermediate. The large difference in the calculated activation barriers (ca. 12.0 and ca. 30.5 kcal mol^{-1} for the Rh and Ir systems, respectively) agrees with the experimental observation, for related systems, of oxidatively induced ethane elimination when M = Rh, whereas the related Ir systems prefer to decompose by alternative pathways.

Keywords: C–C activation · C–H activation · density functional calculations · elimination · spin crossover

Introduction

It is now well appreciated that organometallic reactions may involve intermediates in a different spin state than the reagents and products.[1–5] For instance, species with two unpaired electrons (triplet states) may be generated from diamagnetic reagents, and species with three unpaired electrons (quartet states) may originate from radical-like 17-electron reagents. Therefore, these reactions are characterized by spin-crossover phenomena, with important consequences in terms of reaction rates and selectivities. Recently, we examined the oxidative addition of C–H bonds to triplet 16-electron fragments, notably the reaction of methane with $[Cp_2M]$, $[Cp^*_2M]$ ($Cp^* = \eta^5$-C_5Me_5) and *ansa*-$[CH_2(C_5H_4)_2M]$ (M = Mo, W)[6,7] and the reaction of ethylene with $[CpIr(PH_3)]$.[8] From these studies, it is apparent that proper rationalization of particular experimental observations (notably the relative rates of H/D scrambling and CH_4 elimination for the Group 6 metallocenes,[9–11] and coordinative versus oxidative addition selectivity for the iridium system[12]) could be achieved only through the explicit calculation of the so-called minimum-energy crossing points (MECPs),[13–17] namely, the points along the reaction coordi-

[a] A. Petit, Dr. P. Richard
Laboratoire de Synthèse et d'Electrosynthèse Organométalliques
Faculté des Sciences "Gabriel", Université de Bourgogne
6 Boulevard Gabriel, 21000 Dijon (France)

[b] Prof. I. Cacelli
Dipartimento di Chimica e Chimica Industriale
Università di Pisa, Via Risorgimento 35, 56126 Pisa (Italy)

[c] Prof. R. Poli
Laboratoire de Chimie de Coordination, UPR CNRS 8241
205 Route de Narbonne, 31077 Toulouse Cedex (France)
Fax: (+33) 5615-53003
E-mail: poli@lcc-toulouse.fr

 © 2006 Wiley-VCH Verlag GmbH & Co. KGaA, Weinheim

nate where the system can be thought of as crossing from one potential energy surface (PES) to the other.

Amongst the most thoroughly investigated systems for the oxidative addition of hydrocarbon C–H bonds are the Group 8 $[CpM(PR_3)]$ 16-electron fragments (M = Rh, Ir).[18,19] These species are typically generated in situ by photolysis of $CpM(PR_3)H_2$ or by thermolysis of $[CpM(PR_3)(R)(H)]$ precursors with elimination of H_2 or RH, respectively.[20–25] This process has also been extensively investigated by computations for the Rh and Ir systems,[26–29] which indicate that the 16-electron intermediates undergoing oxidative addition adopt a triplet ground state. None of the previously reported investigations, however, have examined the details of the crossing region and how these may affect the reaction rate. We previously presented a computational investigation of [CpCoL] ($L = PH_3$, C_2H_4),[30] but this focussed on the ligand-addition processes and did not address the possible oxidative addition of C–H bonds.

A related phenomenon that has attracted our attention is the oxidatively induced decomposition of 18-electron $[L_nM(CH_3)_2]$ (M = Rh, Ir) complexes, namely, $[Cp^*M(PPh_3)(CH_3)_2]$,[31–33] $[L_3Rh(CH_3)_3]$ (L_3 = 1,4,7-trimethyl-1,4,7-triazacyclononane),[34] and $[Cp^*M(Me_2SO)(CH_3)_2]$,[35] and especially the remarkably different outcomes for the two metals. Whereas oxidation of the Rh complex induces reductive elimination of ethane for all the above-mentioned compounds, the corresponding process in the Ir analogues leads to a different decomposition pathway featuring elimination of methane. Mechanistically, the decomposition process in the Rh systems seems to be controlled by simultaneous breaking of the two metal–carbon bonds, whereas the Ir systems seem to decompose by rate-determining bond-formation processes.[35] However, the oxidation of $[Cp^*Ir(PMe_3)(CH_3)H]$ results in exclusive elimination of methane, and an oxidatively induced reductive elimination pathway was suggested to rationalize this behavior.[32]

From the energetic point of view, the reduced system favors the oxidative addition product $[M^{III}(R)(H)]$ for both Rh and Ir, whereas the oxidized system favors the reductive elimination product $[M^{II}]^+$ in combination with the formation of C–C bonds for Rh and C–H bonds for Ir. To our knowledge, the C–H or C–C activation process involving the cationic system has not been previously examined from the computational standpoint. A reductive elimination process on a 17-electron complex leads to a 15-electron intermediate, with the potential involvement of a quartet PES. We considered it of interest to investigate and understand the factors determining the different energetic preferences of the neutral and cationic complexes, which lead to different decomposition pathways for the cationic dimethyl Rh and Ir systems. For these reasons, we carried out calculations on three model systems: 1) $[CpM(PH_3)] + CH_3–H$ for M = Co, Rh, Ir; 2) $[CpM(PH_3)]^+ + CH_3–H$ for M = Rh, Ir; 3) $[CpM(PH_3)]^+ + CH_3–CH_3$ for M = Rh, Ir. The inclusion of the experimentally less relevant Co system is interesting from the fundamental standpoint for a detailed examination of trends in bond energetics and metal electronic parameters (orbital gap, pairing energy).

Results and Discussion

Methane C–H oxidative addition to 16-electron $[CpM(PH_3)]$: This is the first comparative study of this reaction for all three Group 9 metal complexes and the first reporting all critical points along the reaction coordinate, including the MECP. Previous investigations have addressed the thermodynamics of methane addition to the Rh and Ir fragments by using LCAO-HFS,[26] RHF,[27] MP2[27,28] and MP4(SDTQ),[28] as well as selectivity issues for the oxidative addition of propane and cyclopropane to the same fragments using B3LYP.[29] $[CpCo(PH_3)]$ has also been previously examined theoretically by B3LYP, but the reaction with methane was not addressed.[30] The present study also makes use of the B3LYP functional within the DFT methodology. All relevant critical points of the reaction coordinate for both singlet and triplet PES have been calculated for the three metal systems and are shown in Figure 1. Selected geometric parameters for the optimized structures are listed in Table 1.

The 16-electron $[CpM(PH_3)]$ fragment is more stable in the triplet state for all metals. The singlet–triplet gap is very similar for the Rh and Ir systems, whereas it is much greater for the Co system. These calculated gaps are close to those previously calculated at similar computational levels.[36] We do not intend to stress the accuracy of the various methods for estimation of this gap, a topic that currently attracts considerable attention. Rather, we focus on the trends shown by this gap as the metal is changed down the group and on the physical reasons that allow this trend to be rationalized. Neither do we dwell on the optimized geometries of the 16-electron fragments, since these have also been extensively discussed in the previous reports cited above.

The interaction of methane with the triplet fragment is repulsive in all cases. This is quite expected, since the C–H bond of methane is a very weak donor and does not effectively compete with the ligands that are already present in the coordination sphere in terms of providing electronic saturation to the metal center.[4,5] A similar situation was demonstrated for the repulsive addition of N_2 to triplet $[CpMoCl(PH_3)_2]$ (whereas CO addition is attractive),[37,38] for the repulsive addition of methane to the triplet metallocenes of Mo and W,[6] for the repulsive addition of H_2 to spin triplet FeL_4 substrates (L = CO, phosphane),[39] and more recently for the repulsive addition of H_2 to $[W\{N(CH_2CH_2NSiMe_3)_3\}H]$.[40] Methane addition, on the other hand, is attractive to singlet $[CpM(PH_3)]$ for all metals. Again, this is expected because suitable orbitals in terms of energy, symmetry and occupancy are available in the singlet fragment for establishment of the two key bonding interactions with the methane ligand: σ donation of the C–H bonding electrons into the metal empty orbital and π backbonding from a metal lone pair to the empty C–H antibonding orbital.

 © 2006 Wiley-VCH Verlag GmbH & Co. KGaA, Weinheim

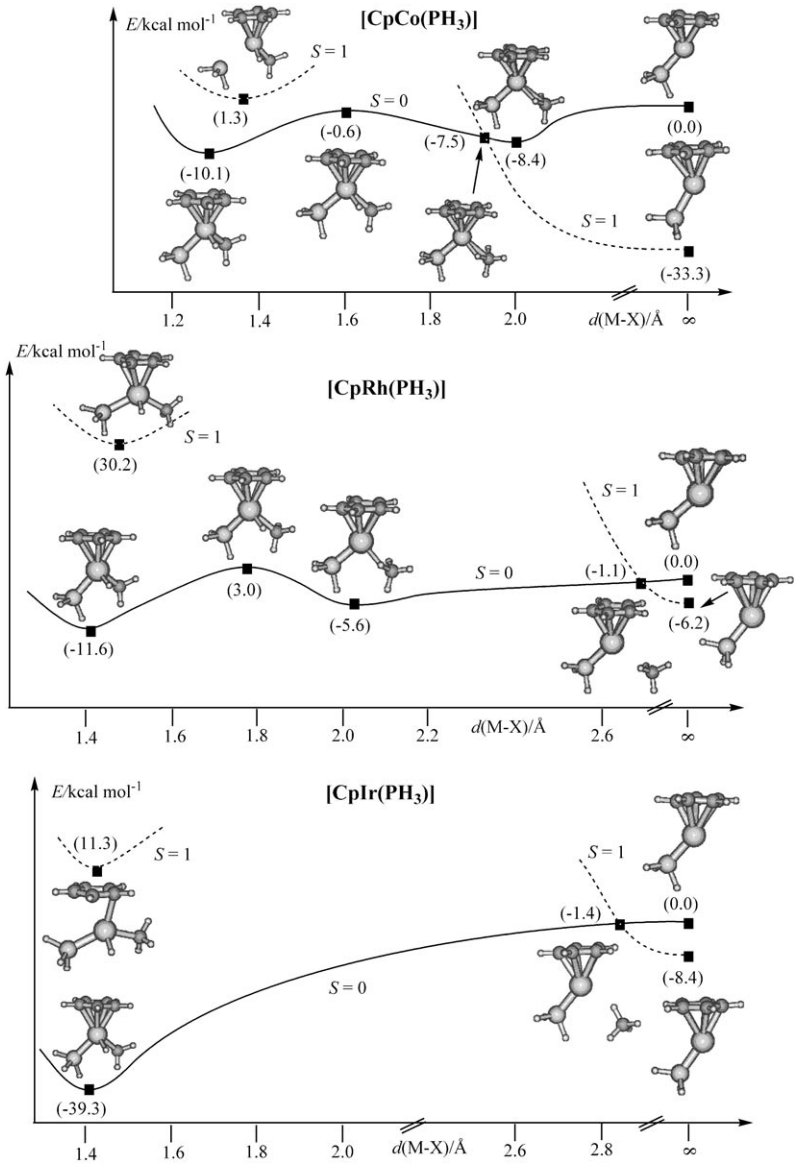

Figure 1. Reaction coordinate for C–H oxidative addition of methane to [CpM(PH_3)] (M = Co, Rh, Ir). The M–X distance on the abscissa is the distance between the metal center and the midpoint of the C–H bond.

For the cobalt and rhodium systems, methane addition on the singlet PES leads to a local minimum that corresponds to the σ-CH_4 complex. Somewhat unexpectedly, the interaction energy is slightly greater for cobalt ($-8.4\,kcal\,mol^{-1}$) than for rhodium ($-5.6\,kcal\,mol^{-1}$). The latter value is close to those previously calculated at other computational levels. Contrary to some of the previously reported investigations,[26,27] but in analogy to others,[28] we could not locate a stable σ-complex minimum for the iridium system. Such a local minimum, if it exists, is likely to have a very low barrier to oxidative addition (see below). The optimized geometries of the Co and Rh σ-CH_4 complexes are similar, with the interacting C–H bond lying approximately parallel to the Cp plane. The M–X distance (see Table 1) is slightly shorter for the Co system, in accordance with the smaller size of the metal. The M–H distances are correspondingly shorter for the Co system, but the difference is much greater for the M–C distance (almost 0.2 Å) than for the M–H distance (ca. 0.08 Å). Thus, it seems that the greater stabilization for the Co system has its origin in the Co–C interaction. The C–H bond is slightly more stretched in the Rh complex.

Continuing on the singlet PES, the σ-CH_4 complex rearranges to the final methyl hydride product via a transition state (for Co and Rh) at about the same energy difference (ca. $8\,kcal\,mol^{-1}$) from the σ-CH_4 complex. The methane fragment is located comparatively much closer to the metal center in the case of Co-TS (the M–X difference is about 0.18 Å). The C–H bond is further stretched relative to the σ-CH_4 complex, and the stretching is more pronounced for the Co system.

The product of oxidative addition, the methyl hydride complex, is energetically more stable than separated methane and singlet 16-electron fragment for all three systems, but this stabilization is much greater for Ir (almost $40\,kcal\,mol^{-1}$) than for the other two metals (ca. 10 and $12\,kcal\,mol^{-1}$ for Co and Rh, respectively). The very small energy difference between the oxidative additions to the singlet Co and Rh complexes may seem surprising when considering that homolytic bond strengths generally increase down a group of transition metals. However, the energetics of this process can formally be split into three components: 1) homolytic rupture of the CH_3–H bond; 2) promotion energy from the lowest energy singlet to an excited singlet (and not triplet, as other authors have often proposed) in which the two electrons used for M–H and M–CH_3 bonding are located in two different orbitals; and 3) formation of the M–H and M–CH_3 bonds. The third component is expected to be less exoergic for Co, but the second should be comparatively less endoergic because the Coulombic repulsion is greater for the less diffuse 3d orbitals.[36] The same phenomenon is responsible for the greater triplet–singlet gap for Co relative to Rh. On going down further to Ir, the strength of the Ir–H and Ir–CH_3 bonds continues to increase, whereas the energetic cost of electronic

 © 2006 Wiley-VCH Verlag GmbH & Co. KGaA, Weinheim

Table 1. Selected distances [Å] and angles [°] for the optimized structures shown in Figure 1.

Molecule[a]	M–X[b]	M–CNT[c]	M–P	M–H	M–C	C–H	CNT-M-P	CNT-M-H	CNT-M-C
$Co(CH_3)(H)$	1.290	1.798	2.157	1.446	1.977	2.310	133.66	123.75	125.62
Co-TS	1.602	1.793	2.165	1.448	2.040	1.500	131.84	131.87	129.74
Co-MECP	1.928	1.750	2.131	1.659	2.312	1.153	133.43	133.68	128.17
$Co(\eta\text{-}CH_4)$	2.034	1.782	2.154	1.790	2.387	1.120	133.85	129.65	128.47
Co-t		1.915	2.227				142.92		
Co-s		1.753	2.158				141.11		
$Rh(CH_3)(H)$	1.412	2.023	2.247	1.553	2.104	2.388	136.17	125.59	136.17
Rh-TS	1.786	2.023	2.246	1.587	2.224	1.474	133.97	133.63	130.45
$Rh(\eta\text{-}CH_4)$	2.148	2.011	2.232	1.842	2.561	1.200	133.91	133.10	131.56
Rh-MECP	2.691	2.027	2.274	2.384	3.067	1.101	135.67	126.05	125.89
Rh-t		2.045	2.305				138.75		
Rh-s		1.990	2.231				138.42		
$Ir(CH_3)(H)$	1.424	1.992	2.232	1.580	2.122	2.425	135.03	126.56	124.48
Ir-MECP	2.838	1.967	2.222	2.346	3.350	1.106	140.80	123.01	132.43
Ir-t		2.002	2.238				140.34		
Ir-s		1.954	2.205				144.24		

[a] The symbol M (Co, Rh, Ir) is used to represent the $CpM(PH_3)$ fragment; s = singlet; t = triplet; TS = transition state; MECP = minimum-energy crossing point. [b] X = midpoint of the H_3C–H vector. [c] CNT = cyclopentadienyl ring centroid.

promotion remains approximately the same as for Rh, since the Rh 4d and Ir 5d orbitals do not differ greatly in size.

Relative to the σ-CH_4 complex, the methyl hydride isomer is stabilized to a greater extent for Rh (ca. 6 kcal mol^{-1}) than for Co (ca. 1.7 kcal mol^{-1}). Relative to the triplet ground state of the 16-electron fragment, the oxidative addition process is highly endoergic for Co, only slightly exoergic for Rh, and strongly exoergic for Ir. For this reason, the oxidative addition of hydrocarbons occurs for the Ir and Rh systems (with a greater bond selectivity for the Rh system, as previously discussed),[29] whereas it has not been observed for the Co system.

From the point of view of the reverse reductive elimination process, the transition state leading to the σ-CH_4 complex is located at relatively low energy (9.5 kcal mol^{-1} for Co, 14.6 kcal mol^{-1} for Rh). In this respect, the Co and Rh PESs are rather similar. The MECP leading to the triplet surface, however, is located at very different positions in the two cases. For the Co system, it is located very near the σ-CH_4 complex, and the two geometries are very similar (see Figure 1 and Table 1). In fact, crossing at the MECP occurs earlier (at a Co–X distance of 1.93 Å) than the σ-methane minimum (Co–X 2.06 Å), and it can consequently occur quite readily. Reductive elimination of methane would not in any way be affected by the need to change spin surface. The reaction is solely dependent on the low barrier for rearrangement to the σ-CH_4 complex along the singlet surface. According to this picture, a hypothetical [CpCo-(PR'_3)(R)(H)] species is predicted to be unstable relative to reductive elimination of the alkane. Indeed, no stable compounds with this stoichiometry appear to be known in the literature. Any such compounds would readily decompose to the alkane and triplet $[CpCo(PR'_3)]$, which would then undergo further transformation into stable products. Corresponding dialkyl complexes, however, are known and do not exhibit a strong tendency to reductively eliminate ethane, presumably for kinetic reasons: the energy barrier to C–C bond formation is likely to be much higher than that associated with C–H bond formation, shown in Figure 1 (see comparison of C–H and C–C reductive elimination barriers for the oxidized Rh and Ir systems below). Reaction intermediates of type $[CpCo(PR_3)]$ have been investigated,[41,42] but no evidence for activity in C–H oxidative addition processes has ever been presented to the best of our knowledge, in contrast to similar unsaturated derivatives of type [CpCo-(olefin)].[43–45]

For the Rh system, the MECP is located at much longer Rh–X distance and its geometry resembles much more that of the separated $[CpRh(PH_3)]$ and CH_4 fragments. The energy of this MECP is only slightly lower than that of the sum of the singlet fragments, and lower than that of Rh-TS. Thus, even though the σ-CH_4 complex is expected to have a longer lifetime relative to the Co case, the reductive elimination process is still energetically controlled by the transition state along the singlet PES. From the experimental point of view, alkyl hydride complexes of type $[CpRh(R)(H)(PR'_3)]$ are unstable and decompose rather readily by reductive elimination, though σ-alkane intermediates have been shown to be involved, in certain cases, during the isomerization of isotopically labeled products.[22,46]

Finally, reductive elimination of methane from [CpIr-$(PH_3)(CH_3)(H)$] proceeds without intermediate (according to the calculations), through a relatively high energy MECP which is located at a long Ir–X distance and close in energy to the separated methane and singlet $[CpIr(PH_3)]$ fragments. This situation is topologically similar to the crossover region for the Rh case, but the optimized geometry for Ir-MECP is different than that of Rh-MECP, with one C–H bond pointing at the Ir center in an end-on fashion rather than in a side-on fashion (see Figure 1). This calculation agrees with the experimental evidence that alkyl hydride complexes are thermally much more robust for Ir than for Rh.[25] There is some experimental evidence for the intermediacy of σ-alkane complexes during the reductive elimination process (notably, a competitive isotope scrambling process during

 © 2006 Wiley-VCH Verlag GmbH & Co. KGaA, Weinheim

the thermolysis of [Cp*Ir(PMe_3)(D)(C_6H_{11})]).[25] It is possible that the shape of the PES around the σ-alkane complexes is sensitive to the coordination sphere, so that a local minimum exists for the real compound but not for the model system used for the calculations. The shape of the PES is also likely to depend on the computational level. As mentioned above, a minimum was indeed found at other levels.[26,27] At any rate, this minimum is likely to be a rather shallow one, with very low barriers to oxidative addition and to scrambling.

Relative stability of spin states for 16-electron $CpM(PH_3)$ and 15-electron $[CpM(PH_3)]^+$: orbital and pairing-energy factors: Removal of one electron from the 16-electron $[CpM(PH_3)]$ complexes produces the corresponding cations in two possible spin states: doublet and quartet. Figure 2

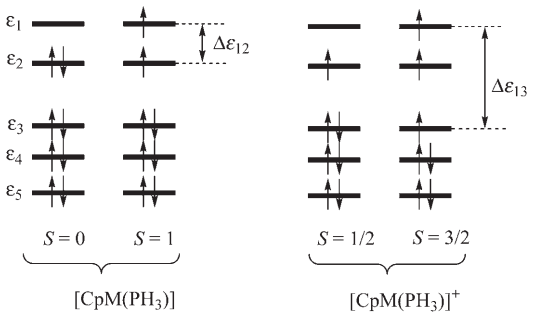

Figure 2. The qualitative energy diagram for both spin states in the neutral and cationic complexes, $[CpM(PH_3)]$ and $[CpM(PH_3)]^+$, respectively, limited to the five d-based metal orbitals for the d^8 or d^7 electronic configuration of Co^I and Co^{II}, respectively.

shows the qualitative energy diagram for both spin states in the neutral and cationic complexes, limited to the five d-based metal orbitals for the d^8 (neutral system) or d^7 (cationic system) electronic configuration of Co^I and Co^{II}, respectively. The optimized energies and key geometrical parameters of all complexes are listed in Table 2.

Table 2. Selected distances [Å], angles [°] and relative energies [kcal mol^{-1}] for the optimized $[CpM(PH_3)]^+$ systems.[a]

Molecule[b]	M–CNT[c]	M-P	CNT-M-P	*E*
Co^+-d	1.83	2.33	134.7	0.0
Co^+-q	1.89	2.42	146.8	−7.4
Rh^+-d	1.91	2.38	132.4	0.0
Rh^+-q	2.12	2.44	143.1	22.7
Ir^+-d	1.88	2.34	135.9	0.0
Ir^+-q	2.08	2.36	144.7	21.3

[a] Values obtained by DFT calculation with an f polarization function on the metal center (see text). [b] The symbol M (Co, Rh, Ir) is used to represent the $CpM(PH_3)$ fragment; d = doublet; q = quartet. [c] CNT = cyclopentadienyl ring centroid.

All oxidized complexes exhibit a similar structure with a bent PH_3 moiety relative to the CNT–M bond. The bending is more accentuated in the doublet state than in the quartet state by about 10°. The Co system behaves differently to the heavier congeners in that the quartet state is most stable. In addition, the doublet cobalt system exhibits a significant spin contamination ($\langle S(S+1)\rangle = 1.18$), corresponding to about 30% contribution of the quartet wave function and about 17% contribution of the quartet density. The rhodium and iridium analogues yield essentially uncontaminated states ($\langle S(S+1)\rangle = 0.76$). Since the Hartree–Fock calculation leads to an even higher value, this feature can not be ascribed to an inadequacy of the DFT method.

The reverse energetic order of the spin states obtained for the cobalt complexes and the marked spin contamination for the doublet induced us to perform more detailed investigations, especially for the doublet cobalt system. First, to feel confident that we are dealing with the absolute minimum for each spin state, we carried out other optimizations starting from different starting geometries and guess densities. Indeed, we have shown in a recent contribution how minima of a quite different nature can be obtained by slight modifications of the guess structure of the Cp_2Cr system.[36] The geometry optimizations for the Co^+-d and Co^+-q systems were repeated by starting the SCF procedure with densities obtained by single excitations on the best Slater determinant (i.e., that giving the best density) and with distorted geometries. However, all our attempts in each spin state led to the same minima reported in Table 2. Only for the quartet Co system was a different structure with an essentially linear CNT-Co-P moiety occasionally optimized. However, this local minimum has a much higher energy than the quartet ground state and even higher than the doublet state reported in Table 2. The similarity of the optimized geometries for the three metal complexes in each spin state gives us further confidence that no lower energy minima exist for these ions.

During the optimization procedures in the doublet state, large spin contaminations were still observed, even for distorted geometries. The calculations, initially performed with a small basis set, were repeated with polarized functions (see Computational Details), which again led to very similar results for all systems in terms of bond lengths, bending angles and quartet–singlet energy differences. Only the results obtained with the larger basis set are shown in Table 2. Second, we inspected the shape and energy of the outer orbitals for all systems (both doublet and quartet states for all metals). All show strong mixing between the metal d orbitals and the Cp π orbitals. In addition, these mixings do not show any regularity, either along the metal series or on going from doublet to quartet. On the other hand, this mixing is not completely unexpected if one considers the differences in ionization potential (IP) of the ligands (12.4 and 9.9 eV for Cp and PH_3, respectively) and the metals (7.9, 7.5 and 9.1 eV for Co, Rh and Ir, respectively). These data lead to the expectation that, as verified in our previous calculations,[36] the outer orbitals will be essentially metal based in the neutral $[CpM(PH_3)]$ systems. For the corresponding cations, on the other hand, one must consider the metal second IP (17 and 18 eV for Co and Rh, respectively). Therefore, the one-electron levels of the metal are predicted to lie at the same energy as (or even below) those of the li-

 © 2006 Wiley-VCH Verlag GmbH & Co. KGaA, Weinheim

gands. This may cause strong orbital mixing, even in the presence of weak bond orders between the metal and the Cp moiety.

We then turned to an analysis of the global properties on the basis of the whole density, rather than on the composition of the outer orbitals, in particular we considered the excess spin ($ES = N_\alpha - N_\beta$) on the ligands and on the metals. As expected, the PH_3 moiety shows a very small ES in view of its closed-shell nature, whereas the metal center carries most of the ES in all cases. The metal ES is 2.4, 2.0 and 2.2 in the Co, Rh and Ir series for the quartet systems, while these values are 1.34, 0.67 and 0.68 for the corresponding doublets. Since $N_\alpha - N_\beta = 1$ for the doublet systems, the Cp ES is negative (-0.34) in the case of Co^+-d, whereas it is about $+0.3$ for Rh^+-d and Ir^+-d. The ES on Co^+-d agrees with the so-called intraatomic Hund's rule,[47] which states that for an atom with a doubly occupied orbital bonded to another atom carrying unpaired electrons (positive ES), the ES is expected to be negative. Figure 3 shows a qualitative

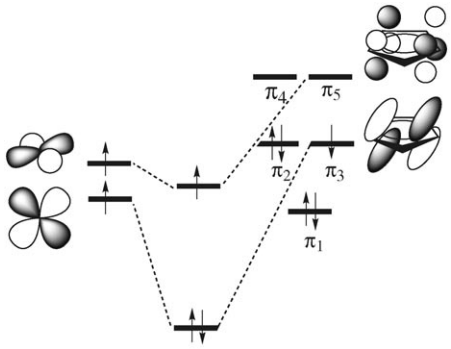

Figure 3. A qualitative fragment orbital analysis of the most relevant covalent interactions between the Cp radical and the 10-electron $[M(PH_3)]^+$ fragment of a d^8 Group 9 metal cation.

fragment orbital analysis of the most relevant covalent interactions between the Cp radical and the 10-electron $[M(PH_3)]^+$ fragment of the d^8 Group 9 metal cation. These are 1) π-type interaction between the singly occupied Cp Huckel-type π_3 orbital and the appropriate metal d orbital, and 2) δ-type backbonding involving the empty Cp Huckel-type π_5 orbital. For the lighter cobalt center, there are two key differences to the heavier congeners. First, both interactions are weaker, and this disfavors full spin annihilation for the π-type interaction. Second, the higher pairing energy for the smaller 3d orbitals stabilizes the $S = 1$ state of the Co^+ center to a greater extent (Hund's rule). Thus, the Co system results in $ES > 1$ on the metal and a slightly negative ES on the Cp ring. For the heavier metal systems, spin annihilation is more effective for the π-type interaction. The reason why the ES on the Cp ring is positive for Rh^+-d and Ir^+-d is related to the greater contribution of the δ-type backbonding interaction.

It is interesting to analyze the reasons for the oxidized $[CpM(PH_3)]^+$ complexes' preferring the lower spin state for M = Rh and Ir (and the higher spin state by a small margin for the Co system), compared to the preference for the higher spin state by all the $[CpM(PH_3)]$ precursors (by a larger margin for the Co system). The relative stabilization of the lower spin state on oxidation is very similar for the three systems, that is, $E_Q - E_D$ for the cation is greater than $E_T - E_S$ for the neutral system by 25.9, 28.9, and 29.7 kcal mol^{-1} for Co, Rh, and Ir, respectively. Using the qualitative concepts of orbital splitting and pairing energy under the monoelectronic approximation (Hartree–Fock theory), the singlet–triplet gap for the neutral system can be expressed as in Equation (1),[48] while the doublet–quartet gap for the cationic system is given by Equation (2).

$$\Delta E_{ST} = E_T - E_S = \Delta\varepsilon_{12} - PI_{ST} = (\varepsilon_1 - \varepsilon_2) - [(J_{22} - J_{12}) + K_{12}] \quad (1)$$

$$\Delta E_{DQ} = E_Q - E_D = \Delta\varepsilon_{13} - PI_{DQ} = (\varepsilon_1 - \varepsilon_3) - [(J_{23} + J_{33} - J_{12} - J_{13}) + (K_{12} + K_{13})] \quad (2)$$

Each expression contains the difference between the one-electron energies of the two orbitals implicated in the electronic promotion process (see Figure 2) and a term corresponding to the pairing energy. The latter contains a difference between an equal number of J integrals [one for Eq. (1), two for Eq. (2)] and a certain number of K integrals. Both J and K integrals have positive values, but J_{ii} values (Coulombic repulsion between electrons in the same orbital) are always greater than J_{ij} values (Coulombic repulsion between electrons in different orbitals); therefore, greater values for J and K integrals lead to a stronger preference for the higher spin state. Conventional wisdom tells us that the J and K values should be greater for the cationic complex than for the neutral one, because the one-electron oxidation process is predicted to lead to a higher effective nuclear charge and thereby to contraction of the electron density around the nucleus. Because of this factor, the preference for the higher spin state should be more pronounced for the cationic system. On the other hand, the relevant orbital gap is greater for the cationic system ($\varepsilon_1 - \varepsilon_3$, see Figure 2), and this factor has an opposite effect to that of the pairing energy. The observation of a greater preference for the lower spin ground state for the cationic systems points to the dominant role of the orbital gap.

In a recent contribution, we presented results for the neutral system[36] which were in qualitative and even semiquantitative agreement with the trend of triplet–singlet gaps down the group ($Co \gg Rh < Ir$). We have now attempted to extend the same analysis to the cationic systems using Equation (2). Unfortunately, as discussed above, going from the neutral to the cationic system results in contraction and lowering in energy of the metal-based orbitals, in such a way that they end up in the same energy region as the M–Cp π orbitals. Therefore, there is extensive mixing between the various orbital contributions, which complicates the J/K analysis. This effect is further accentuated for the related 4+ cations (removal of all unpaired electrons from the

 © 2006 Wiley-VCH Verlag GmbH & Co. KGaA, Weinheim

system is necessary to perform an unbiased J/K analysis).[48] An attempt to apply a localization procedure similar to that of Pipek and Mezey,[49] in order to retrieve essentially metal-based orbitals, gave unexpected results. The lowest unoccupied metal-based orbitals were found to be of s and p character, whereas the d orbitals were pushed to rather high energies. Thus, the unoccupied d orbitals are rather different in the 4+ cation from those observed in the +1 system, because of relaxation effects that upset the orbital ordering and give rise to excessive contractions. In conclusion, this system is unsuitable for the application of qualitative one-electron considerations based on Equation (2). Therefore, we are satisfied with the above qualitative argument, that is, the greater stabilization of the lower spin state for the cationic systems is essentially attributed to the greatly increased energy gap between the relevant orbitals on going from the neutral to the cationic system (Figure 2), which overshadows the expected increase in pairing energy.

Methane C–H reductive elimination from 17-electron $[CpM(PH_3)(H)(CH_3)]^+$: This process has been investigated only for the experimentally more relevant Rh and Ir systems. Since the 15-electron $[CpM(PH_3)]^+$ fragments, like the 17-electron products of methane oxidative addition $[CpM(PH_3)(CH_3)(H)]^+$, adopt a doublet ground state for M = Rh and Ir (see above), the process occurs entirely along the low-spin PES in both cases, without crossover phenomena (Figure 4). It can be safely assumed that no quartet intermediates are involved, because the approach of a weak donor such as the C–H σ-electron density to a high-spin system with no empty metal orbital is expected to be repulsive (see Figure 4), as discussed above in relation to the repulsive approach of methane to triplet $[CpM(PH_3)]$. The calculations were carried out at various fixed points along the coordinate defined by the M–X vector, where X is the midpoint of the C–H axis. Selected geometric parameters for the critical-point structures are collected in Table 3.

It is interesting to compare the results in Figure 2 with the reductive elimination of CH_4 from the neutral singlet $[CpM(PH_3)(H)(CH_3)]$ complexes shown in Figure 1. The process is much more favorable for the cationic complexes than for the corresponding neutral ones. It is endoergic by only 14.6 kcal mol^{-1} for $[CpIr(PH_3)]^+$ relative to 39.3 kcal mol^{-1} for $[CpIr(PH_3)]$, and exoergic by 13.5 kcal mol^{-1} for $[CpRh(PH_3)]^+$ relative to endoergic by 11.6 kcal mol^{-1} for $[CpRh(PH_3)]$. Thus, for each metal, one-electron oxidation makes methane reductive elimination more favorable by about 25 kcal mol^{-1}.

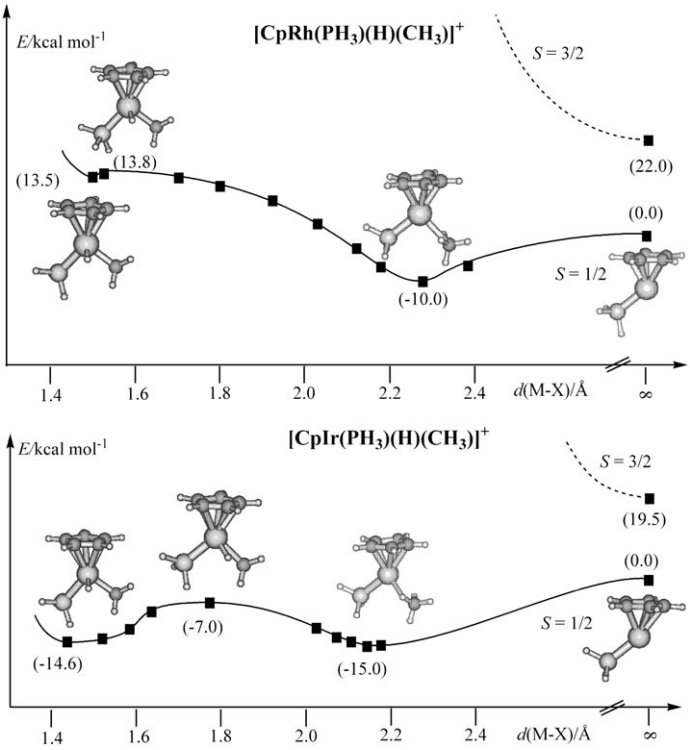

Figure 4. Reaction coordinate for C–H oxidative addition of methane to $[CpM(PH_3)]^+$ (M = Rh, Ir). The M–X distance on the abscissa is the distance between the metal center and the midpoint of the C–H bond. The points marked with energies in parentheses are stationary points. The other points derive from partial optimizations with a constrained C–H distance.

The reductive elimination process proceeds via a σ-CH_4 tautomer. For the cationic Rh system, the methane complex is more stable than the methyl hydride isomer by more than 20 kcal mol^{-1} (cf. less stable by 6 kcal mol^{-1} for the neutral Rh analogue, see Figure 1). Thus, as may be expected, oxidation favors formation of the isomer in which the metal is formally more reduced. In line with Hammond's postulate, the transition state leading from the methyl hydride to the σ-CH_4 complex is much closer in energy and geometry to the starting complex (reactant-like) for the cationic system. This can be readily appreciated by comparing the optimized geometric parameters in Table 3. Indeed, the C–H distance

Table 3. Selected distances [Å] and angles [°] for the optimized structures shown in Figure 4.

Molecule[a]	M–X[b]	M–CNT[c]	M–P	M–H	M–C	C–H	CNT-M-P	CNT-M-H	CNT-M-C
$Rh^+(CH_3)(H)$	1.497	2.009	2.333	1.538	2.097	2.136	135.05	115.22	128.68
Rh^+-TS	1.503	2.008	2.338	1.537	2.100	2.125	135.51	115.21	128.72
$Rh^+(\eta\text{-}CH_4)$	2.283	1.929	2.346	2.150	2.533	1.111	129.62	129.22	135.05
$Ir^+(CH_3)(H)$	1.435	1.997	2.310	1.571	2.093	2.337	135.54	114.02	129.50
Ir^+-TS	1.774	1.955	2.303	1.612	2.210	1.542	132.19	124.24	132.09
$Ir^+(\eta\text{-}CH_4)$	2.138	1.919	2.301	1.925	2.467	1.145	131.28	127.43	134.64

[a] The symbol M (Rh, Ir) is used to represent the $CpM(PH_3)$ fragment; TS = transition state. [b] X = midpoint of the H_3C–H vector. [c] CNT = cyclopentadienyl ring centroid.

 © 2006 Wiley-VCH Verlag GmbH & Co. KGaA, Weinheim

shortens only slightly from 2.136 to 2.125 Å on going from $Rh^+(H)(CH_3)$ to Rh^+-TS, whereas it shortens much more considerably from 2.388 to 1.479 Å on going from Rh(H)-(CH_3) to Rh-TS (see Table 1). For the cationic Ir system, the methane complex and the methyl hydride isomer are essentially isoenergetic, whereas a σ-CH_4 species was not located for the neutral system. The transition state lies about 7.5 kcal mol^{-1} higher than the methyl hydride complex, and its optimized geometry is about midway between those of the two isoenergetic isomers (C–H 1.542 Å). This is again consistent with Hammond's postulate. Under the hypothesis that the putative σ-CH_4 species for the neutral Ir complex enjoys a similar energetic stabilization on going from the neutral to the cationic system, like for the Rh analogue, then the high energy of this putative intermediate along the reaction coordinate shown in Figure 1 would demand a very product-like transition state. Since this intermediate is energetically favorable relative to the product of further methane elimination (positive slope along the reaction coordinate), a local minimum is no longer obtained.

The geometry of the cationic methyl hydride complexes differs considerably from that of the neutral precursors. It is quite distorted relative to the ideal three-legged piano stool, and the distortion consists of widening of the P-M-CH_3 angle. It could more appropriately be described as a four-legged piano stool with a missing leg, such that the hydride ligand is placed in a *transoid* position relative to the missing leg. The CNT-M-H angle is significantly smaller than the CNT-M-CH_3 and CNT-M-PH_3 angles.

One-electron oxidation of $M(H)(CH_3)$ induces more facile reductive elimination of methane. For the rhodium system, the barrier to rearrangement to a methane complex is very low, and this complex, although energetically more stable than the separate methane and 15-electron metal fragment, can easily react with better donor molecules (e.g., the solvent) and by additional redox processes to give thermodynamically stable species. Therefore, our computational study agrees with the literature proposition of oxidatively induced methane reductive elimination from a variety of 18-electron $Rh^{III}(CH_3)(H)$ complexes.[31–35] For the iridium system, the decomposition mechanism of the oxidized methyl hydride complex is essentially the same, in agreement with the experimentally observed selective formation of methane from the oxidative decomposition of [Cp*Ir-$(PMe_3)(CH_3)(H)$].[32] However, the calculations indicate that the higher relative energy of the σ-CH_4 complex imposes a higher energy barrier.

Ethane reductive elimination from 17-electron $[CpM(PH_3)(CH_3)_2]^+$: We now turn to reductive elimination of ethane from $[CpM(PH_3)(CH_3)_2]^+$ for M = Rh and Ir. The endpoint of the process in question is the 15-electron $[CpM(PH_3)]^+$ species already analyzed in the previous two sections. The variable parameter M–X is now defined with X as the midpoint of the C–C axis and, like in the previous section, the entire reaction takes place on the spin doublet surface for both metals. The energetic results and views of the molecular geometries at critical points are shown in Figure 5, while selected geometric parameters for the $[CpM(PH_3)(CH_3)_2]^+$ minimum and for the transition state are given in Table 4.

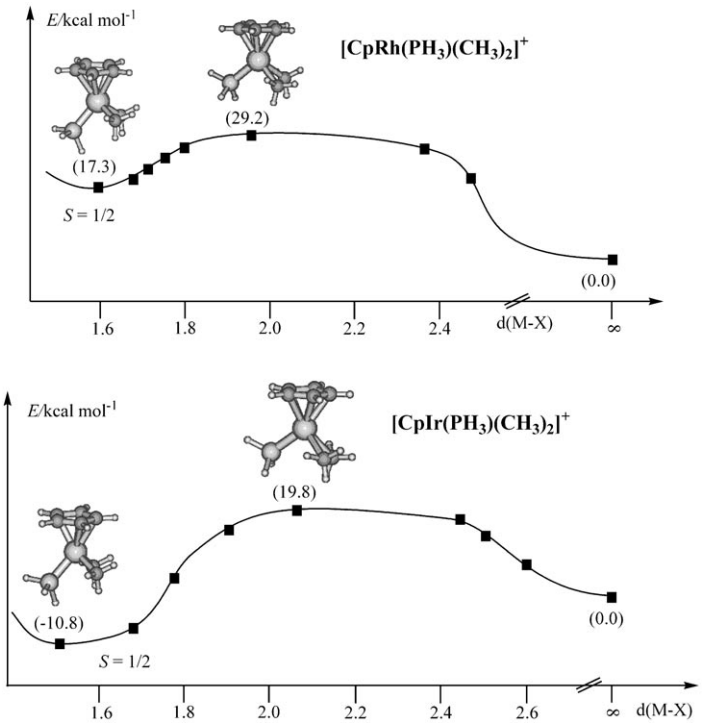

Figure 5. Reaction coordinate for C–C oxidative addition of ethane to $[CpM(PH_3)]^+$ (M = Rh, Ir). The M–X distance on the abscissa is the distance between the metal center and the midpoint of the C–C bond. The points marked with energies in parentheses are the stationary points. The other points derive from partial optimizations with a constrained C–C distance.

The geometry of the oxidative addition product shows the same distortion as the analogous $[CpM(PH_3)(CH_3)(H)]^+$ complexes analyzed above (cf. Tables 3 and 4), with one

Table 4. Selected distances [Å] and angles [°] for the optimized structures shown in Figure 5.

Molecule[a]	M–X[b]	M–CNT[c]	M–P	M–C	C–C	CNT-M-P	CNT-M-C
$Rh^+(CH_3)_2$	1.603	2.031	2.335	2.142	2.741	134.53	113.66
				2.075			127.75
$Rh^+(CH_3)_2$-TS	1.963	1.968	2.344	2.268	2.111	130.22	121.99
				2.189			133.35
$Ir^+(CH_3)_2$	1.514	2.012	2.302	2.148	2.950	133.18	112.57
				2.078			130.04
$Ir^+(CH_3)_2$-TS	2.058	1.947	2.298	2.324	1.983	130.18	124.49
				2.243			134.37

[a] The symbol M (Rh, Ir) is used to represent the $CpM(PH_3)$ fragment; TS = transition state. [b] X = midpoint of the $H_3C–CH_3$ vector. [c] CNT = cyclopentadienyl ring centroid.

 © 2006 Wiley-VCH Verlag GmbH & Co. KGaA, Weinheim

methyl group *transoid* to the phosphane ligand and the second methyl group *cisoid* to the same phosphane ligand (*transoid* to a vacant coordination position) in a pseudo-four-legged piano-stool geometry. This *transoid* methyl ligand exhibits a longer M–CH_3 bond and a smaller CNT-M-CH_3 angle. From the energetic point of view, the picture is very similar to that of the reductive elimination of methane from $[CpM(PH_3)(CH_3)(H)]^+$. The reductive elimination is exoergic by 17.3 kcal mol^{-1} for the Rh system (cf. 13.5 kcal mol^{-1} for the corresponding methane elimination from the methyl hydride) and endoergic by 10.8 kcal mol^{-1} for the Ir system (cf. 14.6 kcal mol^{-1}). Thus, elimination of ethane from the dimethyl complex is more favorable (less unfavorable) than elimination of methane from the methyl hydride complex by about 4 kcal mol^{-1} in both cases. A major difference between the two processes, however, is the absence of a distinct σ-ethane (C–C) complex. A number of other computational studies have addressed C–C bond formation by dialkyl reductive elimination, and in no case was an intermediate σ-C–C complex reported as a stable minimum. The process leads in all cases to C–C bond formation through a high-energy transition state, like in the present case, without stable intermediates or, at most, through an intermediate σ complex that involves one or more C–H bonds, rather than the C–C bond.[50–52]

The energy of the system rises rather quickly from the dimethyl complex to the transition state and then remains high until the ethane molecule is relatively far from the metal center. The transition state is "earlier" for Ir and "later" for Rh, as indicated both by a shorter M–X distance and a longer C–C distances in the former case. This is again in line with Hammond's postulate, given the different reaction energetics. Relative to the transition state for methane reductive elimination from $[CpM(PPh_3)(H)(CH_3)]^+$, however, the energetic barrier is much higher (ca. 12 kcal mol^{-1} higher for the Rh system, ca. 23 kcal mol^{-1} higher for the Ir system). This difference is typical and is generally attributed to the directionality of the sp^3 lobe orbitals.[53–55] Also, the reverse process of C–C oxidative addition is notoriously more difficult than in the case of C–H bonds.[56–58] It seems that an important role is also played by the energetic stabilization of the 3c–2e bonding, which is stronger when the H atom is implicated rather than a methyl group, and leads to the presence of a distinct σ-C–H intermediate in the case of the methyl–hydride elimination process and its absence in the case of the methyl–methyl elimination process. It is notable, however, that the barrier for ethane elimination from $[CpRh(PH_3)(CH_3)_2]^+$ is much lower than that calculated for the same process in the neutral precursor (> 55 kcal mol^{-1}, depending on the computational level).[50] Although the latter calculation was carried out by a quite different method from ours (RHF and RMP2), the large difference is certainly significant. This indicates that, in agreement with the experimental observation, one-electron oxidation kinetically promotes dialkyl reductive elimination. In addition, the process is also promoted thermodynamically, since it is exoergic by 17.3 kcal mol^{-1} for the cation and engoergic by more than 5 kcal mol^{-1} (at the RHF and RMP2 levels) for the neutral complex.[50] Even though the energetics for the neutral system were given relative to the slightly less stable singlet state of the product,[50] and keeping in mind the different computational levels, the difference between the above values can be considered significant.

The transition state exhibits a similar but less pronounced distortion relative to the dimethyl complex. The *cisoid* C atom of the ethane molecule is located at essentially the same position as in the dimethyl complex, whereas the *transoid* one has moved to approach the first one. The relative disposition of the two CH_3 groups in the TS means they already feel the steric H–H repulsion leading to the preferred staggered conformation of the free C_2H_6 molecule.

Coming now to the reactivity of the $[CpM(PPh_3)(CH_3)_2]^+$ (and other isoelectronic) complexes of Rh and Ir, our calculations provide a framework for understanding for the observed difference. For the Rh system, reductive elimination is a thermodynamically favorable process requiring a relatively low activation energy, through a three-center transition state in which the two Rh–C bonds break simultaneously with formation of the C–C bond. Thus, the oxidation of $[CpRh(PPh_3)(CH_3)_2]$ is followed by unimolecular loss of ethane. The absence of a strong rate dependence on the nature of the solvent is consistent with the absence of a dramatic charge redistribution on going from reagent to transition state. Ethane reductive elimination for the dimethyl iridium complex, on the other hand, is thermodynamically unfavorable and requires a higher activation energy (ca. 30 kcal mol^{-1}). Thus, the complex finds other pathways for its thermodynamically favorable decomposition, ultimately leading to different products.

Conclusion

The major outcome of this study is the analysis of how one-electron oxidation modifies the potential energy surfaces for the oxidative addition processes of methane C–H and ethane C–C bonds that link the model $[CpM(PH_3)]$ systems to $[CpM(PH_3)(CH_3)(H)]$ and $[CpM(PH_3)(CH_3)_2]$, respectively, for M = Rh and Ir. Whereas, expectedly, oxidative addition becomes less favorable (or reductive elimination becomes more favorable) on oxidation, other observed variations were less predictable a priori. Many of these variations (e.g., location of the MECP at a much greater M–X distance for the neutral Rh and Ir systems than for the corresponding Co system; the appearance of a well defined σ-CH_4 minimum for the oxidized Ir system but not for the reduced one) can be easily understood on the basis of Hammond's postulate. The comparison of the C–H and C–C activation processes for the oxidized Rh and Ir systems shows that, although the systems are thermodynamically quite similar, the activation barriers are profoundly different because of a much less favorable 3c–2e MC_2 interaction in the C–C activation process relative to the analogous MHC interaction in the C–H activation process. When combined with

 © 2006 Wiley-VCH Verlag GmbH & Co. KGaA, Weinheim

the metal-dependent thermodynamics (reductive elimination favored for Rh, oxidative addition favored for Ir), a reactivity profile in complete agreement with the experimental observations emerges: whereas the [CpRhL(X)(Y)] systems undergo oxidatively induced reductive elimination of X–Y when X = H and Y = CH_3 and also when X = Y = CH_3, the same process from the corresponding [CpIrL(X)(Y)] system is limited to methane. The elimination of ethane from the dimethyl complex is kinetically inaccessible, and other decomposition pathways are favored. Contrary to our initial prediction, these reactions occur entirely on the spin doublet surface without spin crossover, whereas spin-crossover phenomena are involved for the corresponding neutral systems. The reason for the preference of a low-spin (doublet) ground state for the 15-electron $[CpM(PH_3)]^+$ systems, at odds with the preferred high-spin (triplet) ground state for the 16-electron $CpM(PH_3)$ systems, can be rationalized on the basis of the dominant role of orbital energies, in a monoelectronic analytical approach.

Computational Details

The calculations were carried out within the DFT methodology using the hybrid B3LYP functional[59] as implemented in the Jaguar program suite.[60] The LACVP**[61] basis set, consisting of polarized double-zeta basis functions with ECPs on the heavy atoms, was used. In addition, for the calculations involving the oxidative addition/reductive elimination of methane, all the methane H atoms were described more accurately by the extended 6-311G** basis.[62–65] The starting geometries for the various complexes were built from structural parameters available in the Cambridge Crystallographic Database. For the oxidative addition of CH_4 to neutral $[CpM(PH_3)]$ (M = Co, Rh, Ir) only stationary points on the singlet and triplet PESs (local minima and transition states) and the MECP (which is a stationary point within the seam of crossing of the two PESs) were optimized. The transition state on the triplet surface was not optimized, however, as it is not relevant to the chemical process. For the oxidative addition of methane C–H and ethane C–C bonds to cationic $[CpM(PH_3)]^+$ (M = Rh, Ir), the PESs along the reaction coordinates were explored by keeping a representative parameter at various fixed values and freely optimizing all other $3N-7$ internal coordinates. This fixed parameter was chosen as the distance of the bond being formed/broken in the organic molecule (C–H for methane, C–C for ethane). In the Results and Discussion section, however, the coordinate is represented relative to another internal coordinate, namely, the distance between the metal center and the point X located at the center of the fixed C–H or C–C bond, respectively.

The geometry optimization of $[CpMPH_3]^+$ (M = Co, Rh, Ir) was also performed by unrestricted DFT calculations using the B3LYP functional, coupled with LANL2DZ basis set on the metal, and 6-31G* on the carbon, hydrogen and phosphorus atoms. Further polarization functions were added on the H (one p function with exponent $\alpha = 1.1$) and on the metal (one f function) centers. The exponents of the latter were chosen as 2.78, 1.35, and 0.938 for Co, Rh, and Ir, respectively, according to literature optimized values.[66] These calculations were carried out using the Gaussian 03 suite of programs.[67]

MECPs were optimized by using an ad hoc code[17] together with Jaguar. The MECP optimization procedure is based on minimizing a generalized gradient found at any geometry by combining the computed energies and gradients at that point on the two PESs. The gradient contains one term pointing towards the hyperspace in which the two surfaces intersect, and one term pointing towards lower energies within this hypersurface. The mixed Fortran/sheel script code creates Jaguar input files for both spin states at a given geometry, calls Jaguar, extracts energies and gradients from the output files, tests for convergence and cycles.

Acknowledgement

We are grateful to the Conseil Régional de Bourgogne for funds used to upgrade the University's computing facility. R.P. also thanks CINES (Montpellier) and CICT (Project CALMIP, Toulouse) for granting free CPU time.

[1] S. Shaik, D. Danovich, A. Fiedler, D. Schröder, H. Schwarz, *Helv. Chim. Acta* **1995**, *78*, 1393–1407.
[2] D. Schröder, S. Shaik, H. Schwarz, *Acc. Chem. Res.* **2000**, *33*, 139–145.
[3] J. N. Harvey, R. Poli, K. M. Smith, *Coord. Chem. Rev.* **2003**, *238–239*, 347–361.
[4] R. Poli, *J. Organomet. Chem.* **2004**, *689*, 4291–4304.
[5] R. Poli, J. N. Harvey, *Chem. Soc. Rev.* **2003**, *32*, 1–8.
[6] J. C. Green, J. N. Harvey, R. Poli, *Dalton Trans.* **2002**, 1861–1866.
[7] J.-L. Carreón-Macedo, J. N. Harvey, R. Poli, *Eur. J. Inorg. Chem.* **2005**, 2999–3008.
[8] K. M. Smith, R. Poli, J. N. Harvey, *Chem. Eur. J.* **2001**, *7*, 1679–1690.
[9] R. M. Bullock, C. E. L. Headford, K. M. Hennessy, S. E. Kegley, J. R. Norton, *J. Am. Chem. Soc.* **1989**, *111*, 3897–3908.
[10] G. Parkin, J. E. Bercaw, *J. Chem. Soc. Chem. Commun.* **1989**, 255–257.
[11] A. Chernega, J. Cook, M. L. H. Green, L. Labella, S. J. Simpson, J. Souter, A. H. H. Stephens, *J. Chem. Soc. Dalton Trans.* **1997**, 3225–3243.
[12] P. O. Stoutland, R. G. Bergman, *J. Am. Chem. Soc.* **1988**, *110*, 5732–5744.
[13] N. Koga, K. Morokuma, *Chem. Phys. Lett.* **1985**, *119*, 371–374.
[14] A. Farazdel, M. Dupuis, *J. Comput. Chem.* **1991**, *12*, 276–282.
[15] D. R. Yarkony, *J. Phys. Chem.* **1993**, *97*, 4407–4412.
[16] M. J. Bearpark, M. A. Robb, H. B. Schlegel, *Chem. Phys. Lett.* **1994**, *223*, 269–274.
[17] J. N. Harvey, M. Aschi, H. Schwarz, W. Koch, *Theor. Chem. Acc.* **1998**, *99*, 95–99.
[18] W. D. Jones, F. J. Feher, *Acc. Chem. Res.* **1989**, *22*, 91–100.
[19] R. G. Bergman, *J. Organomet. Chem.* **1990**, *400*, 273–282.
[20] A. H. Janowicz, R. G. Bergman, *J. Am. Chem. Soc.* **1982**, *104*, 352–354.
[21] A. H. Janowicz, R. G. Bergman, *J. Am. Chem. Soc.* **1983**, *105*, 3929–3939.
[22] R. A. Periana, R. G. Bergman, *J. Am. Chem. Soc.* **1986**, *108*, 7332–7346.
[23] W. D. Jones, F. J. Feher, *J. Am. Chem. Soc.* **1982**, *104*, 4240–4242.
[24] W. D. Jones, F. J. Feher, *J. Am. Chem. Soc.* **1986**, *108*, 4818–4819.
[25] J. M. Buchanan, J. M. Stryker, R. G. Bergman, *J. Am. Chem. Soc.* **1986**, *108*, 1537–1550.
[26] T. Ziegler, V. Tschinke, L. Fan, A. D. Becke, *J. Am. Chem. Soc.* **1989**, *111*, 9177–9185.
[27] R. Jiménez-Cataño, M. B. Hall, *Organometallics* **1996**, *15*, 1889–1897.
[28] M.-D. Su, S.-Y. Chu, *J. Phys. Chem. A* **1997**, *101*, 6798–6806.
[29] M.-D. Su, S.-Y. Chu, *Chem. Eur. J.* **1999**, *5*, 198–207.
[30] R. Poli, K. M. Smith, *Eur. J. Inorg. Chem.* **1999**, 877–880.
[31] A. Pedersen, M. Tilset, *Organometallics* **1993**, *12*, 56–64.
[32] A. Pedersen, M. Tilset, *Organometallics* **1994**, *13*, 4887–4894.
[33] P. Diversi, S. Iacoponi, G. Ingrosso, F. Laschi, A. Lucherini, C. Pinzino, G. Uccello-Barretta, P. Zanello, *Organometallics* **1995**, *14*, 3275–3287.
[34] E. Fooladi, M. Tilset, *Inorg. Chem.* **1997**, *36*, 6021–6027.
[35] E. Fooladi, T. Graham, M. L. Turner, B. Dalhus, P. M. Maitlis, M. Tilset, *J. Chem. Soc. Dalton Trans.* **2002**, 975–982.
[36] R. Poli, I. Cacelli, *Eur. J. Inorg. Chem.* **2005**, *2324–2331*.

 © 2006 Wiley-VCH Verlag GmbH & Co. KGaA, Weinheim

[37] D. W. Keogh, R. Poli, *J. Am. Chem. Soc.* **1997**, *119*, 2516–2523.
[38] V. R. Jensen, R. Poli, *J. Phys. Chem. A* **2003**, *107*, 1424–1432.
[39] J. N. Harvey, R. Poli, *Dalton Trans.* **2003**, 4100–4106.
[40] J.-L. Carreón-Macedo, J. N. Harvey, *J. Am. Chem. Soc.* **2004**, *126*, 5789–5797.
[41] E. R. Evitt, R. G. Bergman, *J. Am. Chem. Soc.* **1980**, *102*, 7003–7011.
[42] A. H. Janowicz, H. E. Bryndza, R. G. Bergman, *J. Am. Chem. Soc.* **1981**, *103*, 1516–1518.
[43] C. P. Lenges, M. Brookhart, B. E. Grant, *J. Organomet. Chem.* **1997**, *528*, 199–203.
[44] C. P. Lenges, M. Brookhart, *J. Am. Chem. Soc.* **1997**, *119*, 3165–3166.
[45] C. P. Lenges, P. S. White, M. Brookhart, *J. Am. Chem. Soc.* **1998**, *120*, 6965–6979.
[46] W. D. Jones, F. J. Feher, *J. Am. Chem. Soc.* **1985**, *107*, 620–631.
[47] A. Szabo, N. S. Ostlund in *Modern Quantum Chemistry*, Revised 1st ed., McGraw-Hill Publishing Company, New York, **1989**, p. 217.
[48] C. Q. Simpson, II, M. B. Hall, M. F. Guest, *J. Am. Chem. Soc.* **1991**, *113*, 2898–2903.
[49] J. Pipek, P. G. Mezey, *J. Chem. Phys.* **1989**, *90*, 4916–4926.
[50] N. Koga, K. Morokuma, *Organometallics* **1991**, *10*, 946–954.
[51] A. Dedieu, *Chem. Rev.* **2000**, *100*, 543–600.
[52] V. P. Ananikov, D. G. Musaev, K. Morokuma, *Organometallics* **2005**, *24*, 715–723.
[53] J. J. Low, W. A. Goddard, III, *J. Am. Chem. Soc.* **1984**, *106*, 8321–8322.
[54] J. J. Low, W. A. Goddard, III, *J. Am. Chem. Soc.* **1984**, *106*, 6928–6937.
[55] N. Koga, K. Morokuma, *Chem. Rev.* **1991**, *91*, 823–842.
[56] R. H. Crabtree, *Chem. Rev.* **1985**, *85*, 245–269.
[57] R. A. Periana, R. G. Bergman, *J. Am. Chem. Soc.* **1986**, *108*, 7346–7355.
[58] M. Gozin, A. Weisman, Y. Ben-David, D. Milstein, *Nature* **1993**, *364*, 699–701.
[59] A. D. Becke, *J. Chem. Phys.* **1993**, *98*, 5648–5652.
[60] Jaguar 6.0, Schrödinger Inc., Portland, Oregon, **1996–2005**.
[61] P. J. Hay, W. R. Wadt, *J. Chem. Phys.* **1985**, *82*, 299–310.
[62] A. D. McLean, G. S. Chandler, *J. Chem. Phys.* **1980**, *72*, 5639–5648.
[63] R. Krishnan, J. S. Binkley, R. Seeger, J. A. Pople, *J. Chem. Phys.* **1980**, *72*, 650–654.
[64] T. Clark, J. Chandrasekhar, G. W. Spitznagel, P. von R. Schleyer, *J. Comput. Chem.* **1983**, *4*, 294–301.
[65] M. J. Frisch, J. A. Pople, J. S. Binkley, *J. Chem. Phys.* **1984**, *80*, 3265–3269.
[66] A. W. Ehlers, M. Boehme, S. Dapprich, A. Gobbi, A. Hoellwarth, V. Jonas, K. F. Koehler, R. Stegmann, A. Veldkamp, G. Frenking, *Chem. Phys. Lett.* **1993**, *208*, 111–114.
[67] Gaussian 03, Revision B.04, M. J. Frisch, G. W. Trucks, H. B. Schlegel, G. E. Scuseria, M. A. Robb, J. R. Cheeseman, J. Montgomery, J. A., T. Vreven, K. N. Kudin, J. C. Burant, J. M. Millam, S. S. Iyengar, J. Tomasi, V. Barone, B. Mennucci, M. Cossi, G. Scalmani, N. Rega, G. A. Petersson, H. Nakatsuji, M. Hada, M. Ehara, K. Toyota, R. Fukuda, J. Hasegawa, M. Ishida, T. Nakajima, Y. Honda, O. Kitao, H. Nakai, M. Klene, X. Li, J. E. Knox, H. P. Hratchian, J. B. Cross, C. Adamo, J. Jaramillo, R. Gomperts, R. E. Stratmann, O. Yazyev, A. J. Austin, R. Cammi, C. Pomelli, J. W. Ochterski, P. Y. Ayala, K. Morokuma, G. A. Voth, P. Salvador, J. J. Dannenberg, V. G. Zakrzewski, S. Dapprich, A. D. Daniels, M. C. Strain, O. Farkas, D. K. Malick, A. D. Rabuck, K. Raghavachari, J. B. Foresman, J. V. Ortiz, Q. Cui, A. G. Baboul, S. Clifford, J. Cioslowski, B. B. Stefanov, G. Liu, A. Liashenko, P. Piskorz, I. Komaromi, R. L. Martin, D. J. Fox, T. Keith, M. A. Al-Laham, C. Y. Peng, A. Nanayakkara, M. Challacombe, P. M. W. Gill, B. Johnson, W. Chen, M. W. Wong, C. Gonzalez, J. A. Pople, Gaussian, Inc., Pittsburgh, PA, **2003**.

Received: July 27, 2005
Published online: December 6, 2005

 © 2006 Wiley-VCH Verlag GmbH & Co. KGaA, Weinheim